International Journal of Engineering

Journal Homepage: www.ije.ir

Experimental Study on Performance of Ductile and Non-ductile Reinforced Concrete Exterior Beam-column Joint

S. Ravikumar*, S. Kothandaraman

Civil Engineering Department, Puducherry Technological University, Puducherry, India

P A P E R I N F O

Paper history:
Received 19 February 2022
Received in revised form 11 March 2022
Accepted 24 March 2022

Keywords:
Beam-Column Joint
Displacement Ductility
Hysteresis Curve
Energy Dissipation
Reinforced Concrete

A B S T R A C T

The purpose of this study is to evaluate the behaviour and the performance of reinforced concrete (RC) exterior Beam-Column Joints (BCJ) experimentally under reverse quasi-static cycle displacement test conducted for ductile and non-ductile detailed reinforcement. Two columns (one upper and one lower) and one beam were used to construct the specimen; the beam end is free, while the other ends are fixed. These specimens were subjected to reverse cyclic quasi-static stress till failure. At each cycle, the hysteresis curve, cracking loads, ultimate loads, deflection of the loaded at the free end of the beam, crack patterns, and failure mechanisms of BCJ were recorded and studied. Additionally, all specimens' energy dissipation and stiffness deterioration were addressed. The experimental results reveal that the ductile joint (DJ) performance is more satisfactory in all the parameters than the non-ductile joint (NDJ). The ultimate load and energy dissipation of DJ is approximately 20% higher than the NDJ. However, expected beam failure occurred in the ductile joint, and the non-ductile joint underwent undesirable joint failure.

doi: *10.5829/ije.2022.35.07a.03*

NOMENCLATURE

L_d	development length in tension	σ_s	Stress in beam bar
f_y	yield stress of bar	τ_{bd}	Design bond stress
LVDT	Linear Variable Differential Transduser	δ_1, δ_2	Elongation/shortening of beam in tension and Compression
μ	Displacement ductility	$\Delta_{u,y}$	Ultimate and Yield displacement
θ	Joint rotation	d	Vertical distance between the transducers
D_n	Damage Index	$K_{i,n}$	Initial Stiffness and n^{th} cycle stiffness

1. INTRODUCTION

Beam-Column Joints (BCJ) are considered a critical element of reinforced concrete (RC) structures, especially in seismic regions. Because of its region transfer the beam load to column member, complex behaviour under seismic force, complicated in construction due to dense reinforcement. The numerous reconnaissance survey on past earthquakes revealed that many RC framed structures were failure because of BCJ failure. During earthquakes, the BCJ undergoes high shear stress through seismic forces, which cause cyclic action. Kassem et al. [1, 2] were discussed all the vulnerabilities of buildings that cause the failure of the structures in earthquake zones. The lateral forces induced the shear stress cause the diagonal cracks at the joints, resulting in joint shear failure. Initially, the beam reinforcement bars yield under earthquake forces, then bars in joint region yields and bond-slip cause the deterioration of joint strength. Joint failure is undesirable as the joint portion is considered part of the column; the column failures cause the global failure of structures. Many experimental and numerical studies were carried out to understand beam-column joint behaviour under seismic forces and influencing parameters of joint strength [3]. Hanson and Connor [4] are pioneers in

*Corresponding Author Institutional Email: srktce@pec.edu (S. Ravikumar)

Please cite this article as: S. Ravikumar, S. Kothandaraman, Experimental Study on Performance of Ductile and Non-ductile Reinforced Concrete Exterior Beam-column Joint, ***International Journal of Engineering, Transactions A: Basics***, Vol. 35, No. 07, (2022) 1237-1245

understanding the behaviour of beam-column joints. The outcome of the research experiment was defined as the horizontal joint shear. Park and Paulay [5, 6] described the joint shear resisting by two mechanisms of strut and truss mechanism. First, the strut mechanism contributed by the diagonal portion of concrete in joint to resist the joint shear; second, the truss mechanism contributed by vertical and horizontal reinforcement in joint through the bond between concrete and reinforcement. Kim and LaFave [7] proposed using these mechanisms to predict the joint shear strength. Some other researchers experimentally investigated beam-column joint behaviour [8, 9]. Based on these research outcomes international code of practice was prepared for design of beam column joints [10]. Kusuhara and Shiohara [11] loaded ten half-scale reinforced concrete beam-column joint sub-assemblages to investigate using statically cyclic loading to acquire essential data, such as stress in yielding bars and joint deformation. It was discovered that the specimen with transverse beams enhanced its narrative shear capacity when the joint was severely damaged.

Additionally, if the joints were severely damaged, the bond actions of beam bars travelling through them remained lower than the bond strength. Megget and Brooke [12] conducted the joint under cyclic loading to simulate seismic force with various anchorage reinforcement detailing standard 90-degree hook and U bar. Inadequate anchoring length of beam bars at external joints resulted in decreased story shear capacity, column reinforcement yielding, and severe joint damage. In all the above-mentioned experimental studies, the performance of various joints was measured in terms of ultimate strength, ductility factor, energy dissipation, stiffness degradation, and joint rotation.

2. MATERIALS

The specimens were cast in M30 grade concrete. Concrete was made using Ordinary Portland Cement (OPC) 43-grade confirming to IS 8112-2013 [13], M-sand, and crushed stone aggregate with a maximum size of 12 mm. Longitudinal reinforcement was provided by reinforcement steel of grade Fe 500 IS 1786-2008 [14], while transverse reinforcement was provided by plain mild steel bars of grade Fe 250 IS 432 Part1-1982 [15]. Potable water was used in the manufacture and curing of concrete. Manual mixing was done in the laboratory. The concrete design mix of materials by weight for a cubic meter of concrete is given in Table 1. Chemical admixture of superplasticizer of 2.5 liter per cubic meter of concrete used to reduce water content in concrete as per design mix. The average compressive strength of a cube of 150x 150 x 150 mm results in an equal 36MPa after 28days of curing.

TABLE 1. Concrete Design Mix per Cubic meter

Material	Cement	Fine Aggregates	Coarse Aggregates	Water
Weight (kg/m^3)	400	710	1170	470

3. DESCRIPTION OF TEST SPECIMENS

Two sets of exterior beam-column joint (BCJ) subassemblies were prepared for testing. First set specimens were designed using the following strong-column weak-beam concept. Murty et al. [16] with ductile detailing as per IS 13920 [17] with full anchorage length and additional close spacing transverse reinforcement. Another set of specimens resembled current construction practice with the limited anchorage length within the depth of beam in insufficient anchorage length and less transverse reinforcement. Beams and columns were designed based on procedures in IS: 456-2000 [18]. The reinforcement details are illustrated in Figure1 and are also given in Table 2.

3. 1. Specimen Designation *Ductile Joint* - This category specimen is designed based on the special moment-resisting frame as a ductile structure for the special ductile joint [14, 15], as shown in Figure 1. Therefore, this category specimen is designed for ductile behaviour, designated as Ductile Joint (DJ). The anchorage length is provided with full required development length in *tension* plus 10 times of bar diameter, i.e. $\mathbf{anchorage\ length = L_d + 10\emptyset}$.

Non-ductile Joint- This category of test specimen resembles current construction practice for joint details with limited anchorage length within the available beam depth, as shown in details. In addition, this category specimen resembles the non-ductile behaviour, designated as Non-Ductile Joint (NDJ). Both the top and bottom bars of the beam had their anchoring lengths extended beyond the inner face of the column, with a 90° bending towards the joint core. Therefore, the following equation is used to calculate the development length under IS: 13920-1993 [19]:

$$L_d = \frac{\emptyset \sigma_s}{4\,\tau_{bd}} \quad (1)$$

where Ld, development length in tension, ∅-diameter of the bar, σs -stress in the bar (equals to 0.87 times of fy yield stress of bar), τbd- bond stress of plain bars in tension depending on the concrete grade, as given in IS 456: 2000 [18].

All control specimens were cast monolithically at one go in a prepared waterproof coated plywood mould for this research. Firstly, the test specimens were demoulded after 24 hours of casting. Then, the specimen was cured for about 28 days. Curing was accomplished by covering

TABLE 2. Reinforcement details

Specimen Name	Column details		Beam details		Anchorage length
	Longitudinal	Transverse	Longitudinal	Transverse	
Ductile Joint (DJ)	4 # 10mm	4 mm dia @ 30 & 60mm c/c	2#10mm @ top & bottom	4 mm dia @ 37.5 & 75mm c/c	(Ld+10ϕ =) 553mm
Non-Ductile Joint (NDJ)		6 mm dia @ 120mm c/c		6mm @ 100mm c/c	Anchored till the depth of the beam.

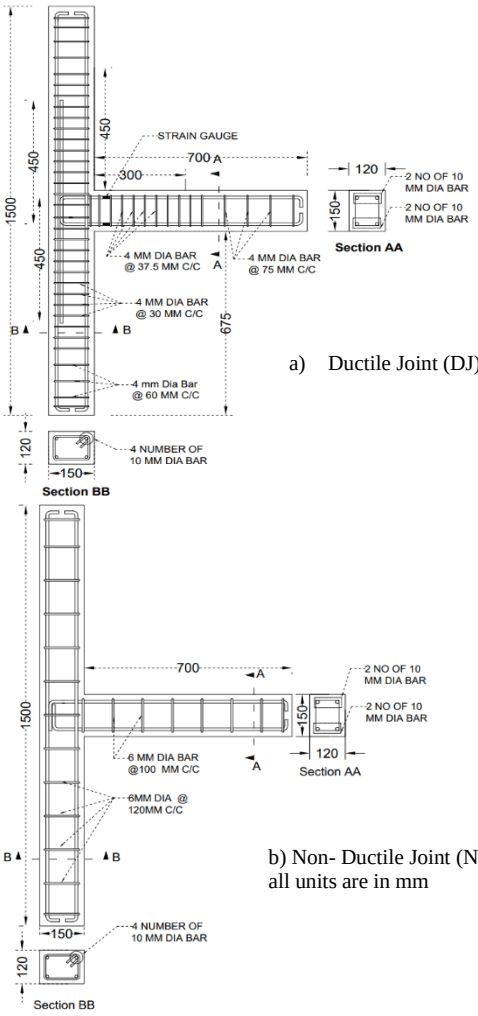

a) Ductile Joint (DJ)

b) Non- Ductile Joint (NDJ), all units are in mm

Figure 1. Test Specimen Reinforcement Details

(a) Prepared Plywood Mould for casting

(b) Prepared specimen during casting and curing

Figure 2. Preparation of mould and specimen

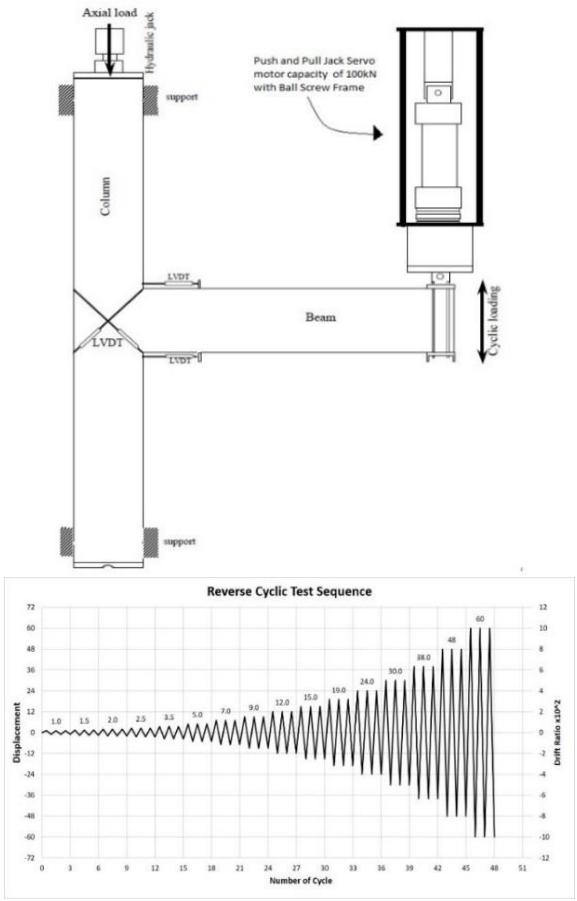

Figure 3. Testing setup and loading sequence

the specimens daily with moist gunny bags at regular intervals, as shown in Figure 2.

4. TEST SETUP AND PROCEDURE

The reverse cyclic test schematic representation of the test setup is shown in Figure 3. Servo-controlled non-hydraulic actuator made exclusive for this project first of

its kind of capacity 100 kN was used for applying cyclic load on the specimen. The peak displacement capacity of the instrument used was ±60 mm. Columns were placed in a vertical position supported on the roller, and the beam was placed in a horizontal position fixed with the actuator. In the present investigation, 10 % capacity of column capacity was applied as the axial load on the column head before starting the test by hydraulic jack of capacity of 500kN to represent the gravity load. The complete setup of the experimental setup is illustrated in Error! Reference source not found..

4. 1. Reverse Cyclic Loading Test Sequence The Push and Pull jack capacity of the 100kN actuator were placed at the beam end to apply the reversible cyclic loading. The main LVDT and loadcell were mounted with an actuator with the reverse cyclic loading history were applied in displacement in the current study, as specified in Figure 3. The reverse cyclic test was conducted in the increment displacements from 1mm to 60mm (0.15 to 9.52 % drift ratio respectively) in 16 number displacements, as shown in Figure 3. Each displacement runs three times a cycle; therefore, 48 displacement cycles are applied to each specimen. The drift ratio is between displacement at the beam end and beam length. The increment of drift ratio is maintained between 1.25 to 1.5.

The downward displacement direction and force (push) have positive signs. On the other hand, the upward displacement direction and force (pull) has negative sign assigned to the loadcell value. All sensors (LVDT and load cell) were linked to a datalogger throughout the test to capture continuous data at regular intervals and store it in the Data Acquisition (DAQ) system. Once the concrete cover began to spall, the four LVDT sensors were removed. However, the data logger is configured to record data continuously without interfering with the primary instrumentation (main LVDT and loadcell) throughout loading and until the last cycle. After that, the test will be terminated either complete test cycle or till the joint collapse, whichever occurs early.

5. EXPERIMENTAL RESULTS AND DISCUSSION

The performance of beam-column joint specimens was evaluated with the following parameters: Hysteresis curve, Ultimate load, Envelope curve, Stiffness degradation, Displacement ductility, Energy dissipation, Damage index, and Crack pattern.

5. 1. Load Deformation Behaviour Hysteresis curve is a graph plotted between the load and displacement at the beam end, and all test specimens were presented in Figure 5 and 6. Additionally, the envelope curves are constructed by connecting the peak load locations of each displacement cycle. The hysteresis curve is used to describe the overall behaviour of elastic and plastic areas. The stable load-displacement curves for ductile and non-ductile joint specimens in the elastic area were obtained during the first loading stage, i.e. at a lower drift level. DJ specimens with stable hysteresis loops illustrate the strength of the link between reinforcement and joint concrete. Pinching began at the very early cyclic loading stage of the NDJ specimens in the downward direction.

The ultimate load of DJ specimen in the positive direction, 13.1kN at the 12 mm displacement 1st cycle, in the negative direction, is 20.5kN at the displacement of 48 mm displacement 1st cycle. The ultimate load of NDJ specimen in the positive direction, 11.6 kN at the 7 mm displacement 1st cycle, in the negative direction, is 15.94 kN at the displacement of 30 mm displacement 1st cycle. The load-carrying capacity of DJ is 20 % higher than NDJ in the positive direction and 11 % higher in the

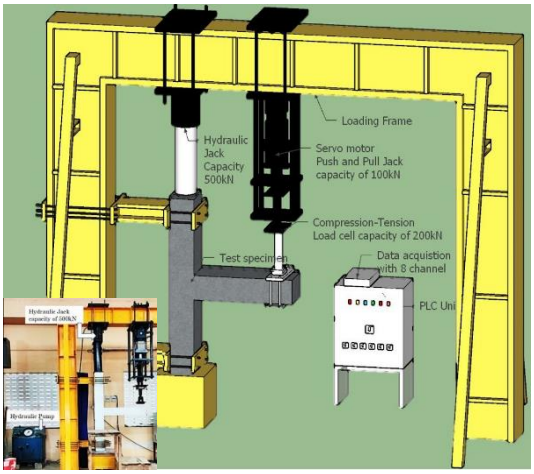

Figure 4. Illustrated the experimental setup

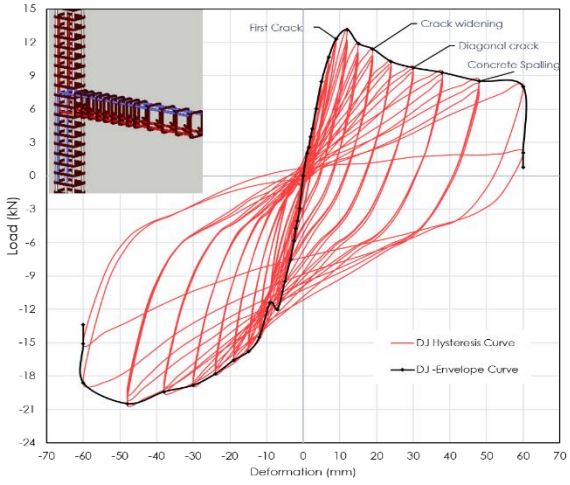

Figure 5. Ductile Joint (DJ) Hysteresis Curve

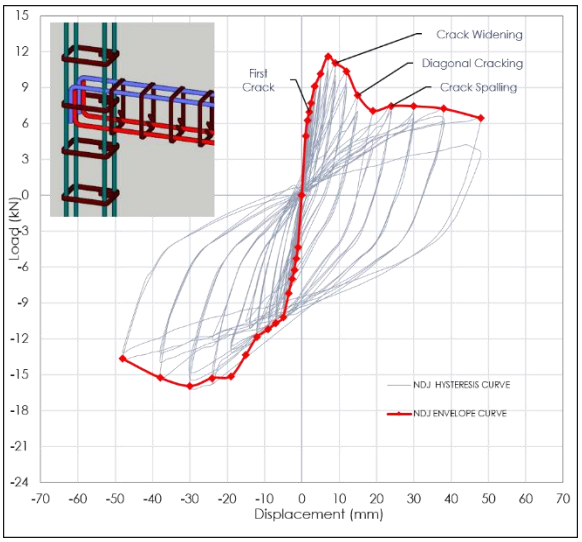

Figure 6. Non-Ductile Joint (DJ) Hysteresis Curve

Negative direction. The DJ has obtained an ultimate capacity of nearly 2% drift ratio, but NDJ obtained at a low drift ratio of 1.1% due to less transverse reinforcement and inadequate anchorage length at the joint.

Figures 5 and 6 show hysteresis behaviour; the DJ specimen has high strength and a fatter hysteresis curve than the NDJ specimen, representing the desirable ductile behaviour. On the other hand, the NDJ specimen has low and sudden significant strength reduction, which is undesirable behaviour of the joint.

5. 2. Crack Pattern and Mode of Failure In the DJ specimen, the first hairline crack occurs at the beam-column joint interface during the 9mm displacement cycle at the load of 12.3kN. Then, multiple hairline cracks occurred at the beam region. Next, the crack at the interface slowly starts widening at the displacement of 19 mm cycle of the load of 11.4kN. Then, the first diagonal cracks appeared in the joint region during the 30mm displacement cycle at the load 9.7kN. Finally, the concrete starts spalling during a 48mm displacement cycle at load 20.5kN. The crack pattern and propagation are presented in Figure 7. From the crack pattern of the DJ specimen, it started with longitudinal bar yielding, then slowly hairlines formed at the joint region, then the cracks at beam and interface widen the beam near joint region. The small concrete spalling started at a 38 mm displacement cycle, and significant concrete spalling occurred at a 60 mm displacement cycle. DJ specimen were cracked pattern increases to beam and beam hinge was developed. It shows that failure mode of DJ specimens beam failure (beam bar yielded before the shear failure at joint).

On the contrary, the NDJ specimen cracks appeared at an early displacement of 2.5 mm at the beam-column joint interface. After that, the beam-column interface crack widened, and concrete started the spalling at 19 mm displacement. For NDJ specimens after the first crack, diagonal cracks were developed as hairlines and slowly started widening with an increment of displacement. NDJ specimen concrete spalling started earlier at 24 mm, beam bars got pulled out of the joint, and bars were cut at 48 mm displacement cycle. So, reverse cycle tests were stopped at this stage. The detailed crack propagation of the first crack, crack widening, diagonal crack formation and concrete spalling out of specimens with respective displacements are shown in Figure 7, and loads are listed in Table 3.

Figure 7 clearly shows that cracks in the DJ specimen were slower than the NDJ specimen from the first crack to concrete spalling. This crack formation in ductile joints is delayed, and the crack widens than the NDJ specimen due to improvement of ductility factor.

5. 3. Displacement Ductility Ductility is defined as the structure's capacity to withstand considerable deformation without losing its significant strength. The structure's ductility helps diffuse the energy generated by

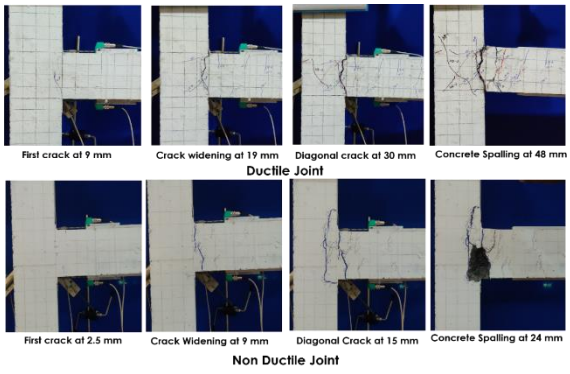

Figure 7. Crack Pattern of Specimen

TABLE 3. Crack Pattern load and displacement

Specimen	First Crack		Crack Widening		Diagonal Crack		Concrete Spalling	
	Δ (mm)	P (kN)	Δ (mm)	P (kN)	Δ (mm)	P (kN)	Δ (mm)	P (kN)
DJ	9	13.4	19	16.6	30	18.8	60	18.6
NDJ	2.5	6.97	9	11.05	15	13.05	24	15.27

an earthquake. The displacement ductility ratio is a standard way to assess the ductility of a structure. The ultimate displacement to yield displacement ratio is the displacement ductility ratio. The ultimate and yield displacement is identified from the hysteresis curve envelope. To evaluate ultimate and yield displacement, many methods were recommended by Park [20].

In this research, the ultimate displacement is found by the ultimate load with significant reduction after the peak load method. The ultimate displacement is defined as a slight reduction in maximum load by 80 % after the peak load (see Figure 8a). The yield displacement is identified by the reduced stiffness equivalent elasto-plastic yield method (see Figure 8b). First, the maximum load point is traced horizontally as a reference; then, a point is marked on the envelope with secant stiffness at 75% of the maximum load (Hu); then, a line is plotted from origin to pass through the respective point to the reference line, with that respective point displacement is yield displacement. The respective ultimate displacement, yield displacement and displacement ductility of the specimens are specified in Table 4.

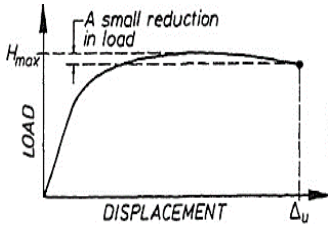

(a) Ultimate displacement

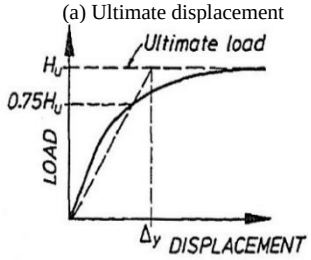

(b) Yield Displacement

Figure 8. a) Ultimate Displacement-Ultimate load Significant load capacity after peak load, b) Yield displacement- reduced stiffness equivalent Elasto-plastic yield [20]

TABLE 4. Displacement Ductility

Specimen Name	Ultimate displacement (Δ_u) mm		Yield Displacement (Δ_y) mm		Displacement Ductility Factor (μ)	
	+	-	+	−	+	−
DJ	23.6	60	8.2	18	2.87	3.33
NDJ	14	49	6	17	2.33	2.88

where, + ve means downward direction displacement, -ve upward direction displacement.

5. 4. Energy Dissipation The area encompassed by the load versus deflection graph (hysteresis curve) was used to calculate the energy dissipated during each cycle. The area included inside each cycle was determined as energy dissipation (kN-mm). The energy dissipation during the first cycle was expected to be about zero for all specimens. However, the energy dissipated throughout a cycle increased when the specimen was supplied with a more significant cyclic load. Figure 9 depicts the rate of increase in energy dissipated for all specimens at each cycle. For specimen DJ, increased energy dissipated at the test start was more significant than increased energy dissipated during the test. The maximum energy dissipated at the 48 mm displacement cycle and was reduced after concrete spalling out. The cumulative energy dissipation increased by 40% for the specimen DJ than the specimen NDJ. The experimental results indicate closed spaced stirrups inside the beam-column connection significantly improved energy dissipation.

5. 5. Stiffness Degradation The stiffness of the beam-column joint under cyclic load can be defined as it resists deformation due to an applied force. Usually, the joint stiffness reduces under cyclic/repeated loading [21]. Figure 10 presents the relationship between beam-column joint stiffness and cycle number for all specimens. The stiffness of beam-column joints under reverse cyclic load is calculated by dividing the peak load by its respective displacement in the experiment. The finding shows that the stiffness of the beam-column junction and the displacement cycle number is inversely related. The degree of damage determines the remaining stiffness. The rigidity of the beam-column joints rises as the fraction of the stirrup's joint increases. The testing results showed that the stirrups enhanced joint shear and load-carrying capacity with less restrained deformations [22]. The stiffness degradation NDJ occurred earlier due

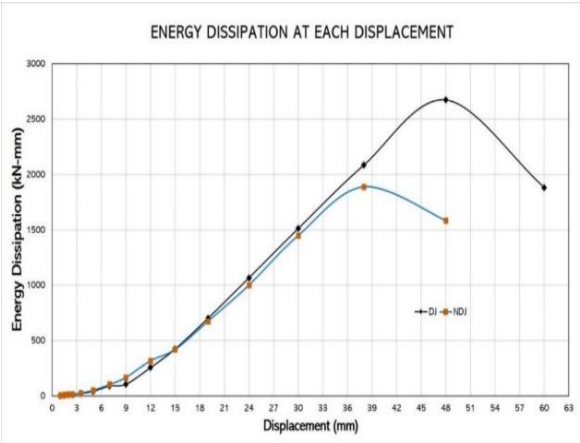

Figure 9. Energy dissipation of respective displacement

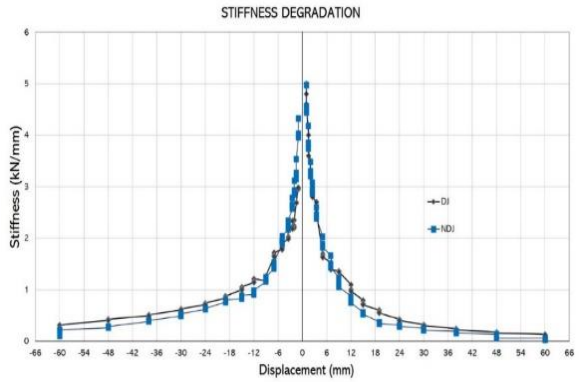

Figure 10. Stffness Degradation

to concrete contribution lost after early cracks, but for the DJ specimen, stiffness was slowly degraded due to its more anchorage length and stirrups at the joint.

5. 6. Damage Index The Damage Index, Dn is a parameter that defines the specimen that sustains the damage through the ratio of its stiffness at a specific cycle to its initial stiffness [23]. Effective confinement of column and beam reduce the damages of specimen [24]. The damage index is found by Equation (2).

$$D_n = 1 - \frac{k_n}{k_i} \quad (2)$$

where ki and kn are the initial stiffness and stiffness at the nth cycle of the specimen, respectively. Figure 11 shows that the NDJ specimen has a large damage index because that section loses the concrete contribution for part to joint stiffness after cracking. NDJ specimens ultimately failed at 48 mm displacement, and DJ did not completely collapse until the last displacement of 60mm.

5. 7. Beam Moment and Rotation Relationship The joint rotations were calculated at the distance of 100mm from the face of the column using the LVDT placed on top and bottom of the beam shown in Figure 12. This portion of the beam undergoes maximum moment and high stress during an increase in the displacement cycle. The joint rotation θ was calculated using the following equation.

$$\theta = \frac{\delta_1 + \delta_2}{d} \quad (3)$$

where, δ_1 is the elongation on the tensile face of the beam, δ_2 is the shortening on the compressive face of the beam, and d is the vertical distance between the transducers (160 mm). The beam rotation angle at 100 mm from the column face, in rad, is plotted against the applied moment for the specimens.

Comparison the beam moment-rotation plots reveal that specimen NDJ (Figure 13) exhibited a much lower rotation before beam yielding (at comparable bending moments) than specimen NDJ for the 100 mm long beam segment from the column face. The decreased stiffness of DJ rebars, on the other hand, resulted in more significant rotations in the DJ-reinforced beam at comparable moments than in the steel-reinforced beam. However, because of the DJ specimen's mainly elastic behaviour, there were relatively few residual deformations in the beam [25]. Furthermore, despite many fractures, the level of damage in the beam for specimens DJ shows less spalling than the NDJ specimen beam.

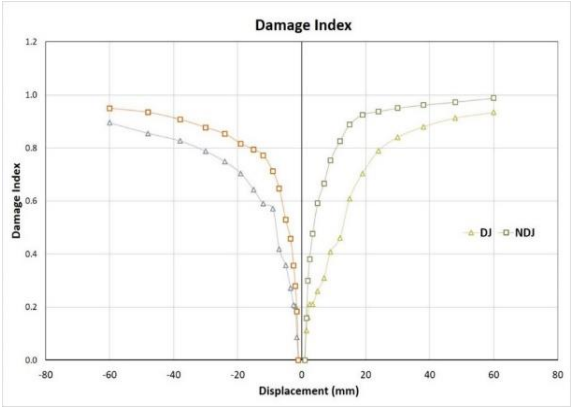

Figure 11. Damage Index

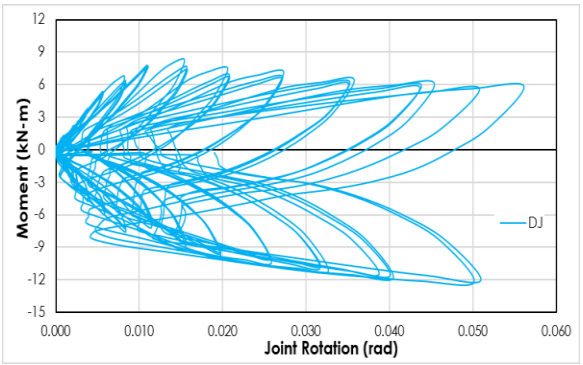

Figure 12. Beam moment Rotation of DJ specimen

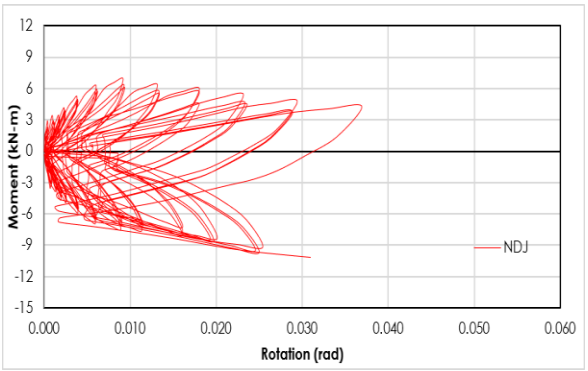

Figure 13. Beam moment Rotation of NDJ specimen

6. CONCLUSIONS

The experimental investigation on the performance of RC beam-column joints subjected reversed cyclic loading, as the simulation of seismic forces. The present experimental study included two exterior reinforced concrete beam-column joint specimens. The displacement cycle was applied at the free end of the beam. The specimens were put through a total of 48 cycles with 16 displacements at each cycle. This research aimed to find the effect of anchorage length of beam reinforcement and the effect of transverse reinforcement on joint performance improvement in terms of the hysteresis curve, envelope curve, crack patterns, mode of failure, and failure. The following findings may be taken from research conducted in this study.

- It was found that for DJ specimens with more stirrups in the joint as ductile detail, the first crack of the joint was delayed, but for NDJ specimens, cracks developed earlier than DJ specimens.
- It was noticed that the hysteresis curve of the DJ specimen was recorded till the last cycle of 60mm displacement without collapse, but NDJ specimens had collapsed at 48 mm displacement cycle.
- Due to insufficient anchorage length of beam bars and no proper anchorage system in the NDJ specimen, the beam bars got pulled out at the higher displacement cycle and caused the joint failure.
- The anchorage length and transverse reinforcement play a significant role in transferring the load and load-carrying capacity of the DJ specimen to 20 % higher than that of the NDJ specimen.
- Energy dissipation capacity is 40% higher for the DJ specimen than that of the NDJ specimen.
- Beam moment versus rotation of beam plots indicated that NDJ resists less moment than DJ specimen with the relative rotation.
- The beam moment versus joint rotation shows the precise formation of plastic hinges in beam for DJ specimen with high deformation, but NDJ specimen has formed failure mechanism of joint.
- This study reveals that closed spaced stirrups plays significant role in the ultimate load capacity and ductility of structure, so it is highly recommended to consider in the beam-column joint design.

7. ACKNOWLEDGEMENTS

The research was financially supported by the AICTE (All India Council for Technical Education) - RPS NDF Grant and Pondicherry Engineering College research funding. The authors gratefully acknowledge these supports.

8. REFERENCES

1. M. M. Kassem, F. M. Nazri, E. N. Farsangi, and B. Ozturk, "Improved Vulnerability Index Methodology to Quantify Seismic Risk and Loss Assessment in Reinforced Concrete Buildings," ***Journal of Earthquake Engineering.*, 2021**.
2. M. M. Kassem, F. Mohamed Nazri, E. N. Farsangi, and B. Ozturk, "Development of a uniform seismic vulnerability index framework for reinforced concrete building typology," ***Jounral of. Build. Engineering***., vol. 47, 2022.
3. S. Ravikumar, S. Kothandaraman, Influencing Parameters of Exterior Reinforced Concrete Beam-Column Joint Shear Strength: A Depth Review of Recent Advances, ***International Journal of Engineering, Transactions B: Applications***, Vol. 35, No. 05, (2022) 931-942. doi: 10.5829/ije.2022.35.05b.09.
4. N. Hanson and H. Conner, "Seismic Resistance of Reinforced Concrete Beam-Column Joints," ***Jounral of Structural. Divison***., vol. 93, no. 5, pp. 533–560, 1967.
5. R. Park and T. Paulay, "Behaviour of reinforced concrete external beam-column joints under cyclic loading," in Proceedings Fifth World Conference on Earthquake Engineering, 1973, p. 10.
6. R. Park and T. Paulay, *Design Concrete Structures*. John Wiley & Sons, New York., 1975.
7. J. Kim and J. LaFave, "Probabilistic joint shear strength models for design of RC beam-column connections," ***ACI Structural jounral***, vol. 105, no. 6, pp. 770–780, 2008.
8. J. Yu and K. H. Tan, "Special detailing techniques to improve structural resistance against progressive collapse," ***Journal of Structural Engineering*** *(United States)*, vol. 140, no. 3, pp. 1–15, 2014.
9. S. Chidambaram and G. Thirugnanam, "Comparative Study on Behaviour of Reinforced Beam-Column Joints with Reference to Anchorage Detailing," ***Journal of Civil Engineering Research,*** vol. 2, no. 4, pp. 12–17, 2012.
10. S. Ravikumar and S. Kothandaraman, "Design of Reinforced Concrete Beam-Column Joint," ***Interantional. Journal of Engineering Trends and Technology***., vol. 70, no. 3, pp. 85–94, 2022. doi:10.14445/22315381/IJETT-V70I3P210
11. F. Kusuhara and H. Shiohara, "Tests of RC Beam-Column Joint with Variant Boundary Conditions and Irregular Details on Anchorage of Beam Bars," ***14th World Conference on Earthquake Engineering,*** pp. 1–8, 2008.
12. L. M. Megget and N. J. Brooke, "Beam-column joint tests with grade 500E reinforcing," no. ***NZSEE conference*** 41, 2004.
13. IS: 8112 – 1989, "Specification for 43 grade Ordinary Portland Cement," ***Bureau of Indian Standard (BIS),*** *Delhi*, p. 17, 2013.
14. IS 1786, "High Strength Deformed Steel Bars and Wires for Concretereinforcement— Specification," ***Bureau of Indian Standard (BIS)***, *New Delhi*, pp. 1–12, 2008.
15. IS 432, "Indian standard specification for mild steel and medium tensile steel bars and hard-drawn steel wire for concrete reinforcement," ***Bureau of Indian Standard (BIS),*** p. 9, 1982.
16. C. V. . Murty and V. V. M. Murty, C. V. R., Rupen, Goswami., A. R. Vijayanarayanan., *Some Concepts Earthquake Behaviour of Buildings*. ***GSDMA***, 2012.
17. IS:13920-2016, "Ductile Design and Detailing of Reinforced Concrete Structures Subjected to Seismic Forces — Code of Practice," ***Bureau of Indian Standard (BIS)***,. *New Delhi*, no. July, pp. 1–121, 2016.
18. IS 456-2000, "Plain and Reinforced Concrete," ***Bureau of Indian Standard (BIS)***. *Dehli*, pp. 1–114, 2000.
19. IS:13920, *Ductile Design and Detailing of Reinforced Concrete Structures Subjected to Seismic Forces*, no. July. ***Bureau of Indian***

Standard (BIS), 1993.

20. R. Park, "Ductility evaluation from laboratory and analytical testing," *Proceedings of **the 9th World Conference on Earthquake Engineering**, 2-9 August*. pp. 605–616, 1988.
21. N. Ganesan, P. V. Indira, and R. Abraham, "Steel fibre reinforced high performance concrete beam-column joints subjected to cyclic loading," ***ISET J. Earthq. Technol.***, vol. 44, no. 3–4, pp. 445–456, 2007.
22. C. Marthong, A. Dutta, and S. K. Deb, "Effect of Cyclic Loading Frequency on the Behavior of External RC Beam-Column Connections," ***Journal of Earthquake Engineering***., vol. 20, no. 7, pp. 1126–1147, 2016.
23. J. Lemaitre and R. Desmorat, *Engineering Damage Mechanics: Ductile, Creep, Fatigue and Brittle Failures*. ***Springer Science & Business Media***, 2006.
24. S. T. Nemati Aghamaleki, M. Naghipour, J. Vaseghi Amiri, M. Nematzadeh, Experimental Study on Compressive Behavior of Concrete-filled Double-skin Circular Tubes with Active Confinement, ***International Journal of Engineering***, ***Transactions A: Basics*** Vol. 35, No. 04, (2022) 819-829
25. T. K. and H. F. Sefatullah Halim, Susumu Takahashi, Toshikatsu Ichinose, Masaomi Teshigawara, "179-192 Amorn Pimanmas," ***Preeda Chaimahawa Journal of Advance Concrete Technology***, vol. 12, no. 4, pp. 146–157, 2014.

Persian Abstract

چکیده

هدف از این مطالعه ارزیابی رفتار و عملکرد اتصالات تیر–ستون خارجی (BCJ)بتن مسلح (RC)تحت آزمایش جابجایی چرخه شبه استاتیک معکوس انجام شده برای آرماتورهای دقیق شکل‌پذیر و غیر شکل‌پذیر است. برای ساخت نمونه از دو ستون (یکی بالا و دیگری پایین) و یک تیر استفاده شد. انتهای تیر آزاد است، در حالی که انتهای دیگر ثابت است. این نمونه ها تا زمان شکست تحت تنش شبه استاتیکی چرخه ای معکوس قرار گرفتند. در هر چرخه، منحنی پسماند، بارهای ترک، بارهای نهایی، انحراف بارگذاری شده در انتهای آزاد تیر، الگوهای ترک و مکانیسم‌های شکست BCJ ثبت و مورد مطالعه قرار گرفتند. علاوه بر این، تمام اتلاف انرژی و زوال سفتی نمونه ها مورد بررسی قرار گرفت. نتایج تجربی نشان می‌دهد که عملکرد اتصال شکل‌پذیر (DJ)در تمام پارامترها نسبت به اتصال غیر شکل‌پذیر (NDJ)رضایت‌بخش‌تر است. بار نهایی و اتلاف انرژی DJ تقریباً ۲۰٪ بیشتر از NDJ است. با این حال، شکست تیر مورد انتظار در اتصال شکل‌پذیر رخ داد و اتصال غیر شکل‌پذیر دچار شکست مفصلی نامطلوب شد.